Propagating fronts in the complex Ginzburg-Landau equation generate fixed-width bands of plane waves

Matthew J. Smith*
Microsoft Research, 7 J.J. Thompson Avenue, Cambridge CB3 0FB, United Kingdom

Jonathan A. Sherratt†
Department of Mathematics and Maxwell Institute for Mathematical Sciences, Heriot-Watt University, Edinburgh EH14 4AS, United Kingdom

(Received 30 April 2009; revised manuscript received 1 September 2009; published 20 October 2009)

Fronts propagating into an unstable background state are an important class of solutions to the cubic complex Ginzburg-Landau equation. Applications of such solutions include the Taylor-Couette system in the presence of through flow and chemical systems such as the Belousov-Zhabotinskii reaction. Plane waves are the typical behavior behind such fronts. However, when the relevant plane-wave solution is unstable, it occurs only as a spatiotemporal transient before breaking up into turbulence. Previous studies have suggested that the band of plane waves immediately behind the front will grow continually through time. We show that this is in fact a transient phenomenon and that in the longer term there is a fixed-width band of plane waves. Moreover, we show that the phenomenon occurs for a wide range of parameter values on both sides of the Benjamin-Feir-Newell and absolute instability curves. We present a method for accurately calculating the parameter dependence of the width of the plane-wave band facilitating future experimental verification in real systems.

DOI: 10.1103/PhysRevE.80.046209 PACS number(s): 05.45.−a, 02.70.−c, 47.54.−r

I. INTRODUCTION

The cubic complex Ginzburg-Landau equation (CGLE) is one of the most studied nonlinear equations in physics [1]. It is a generic model for weakly nonlinear spatially extended oscillatory media arising as the amplitude equation near a supercritical Hopf bifurcation [2]. An important problem in such systems is front propagation into an unstable state and the CGLE has been fundamental to the study of this problem in contexts including the Taylor-Couette system in the presence of through flow [3,4] and chemical systems such as the Belousov-Zhabotinskii reaction [5]. Here we report on, and explain, a previously unrecognized phenomenon associated with such front propagation: a fixed-width band of plane waves behind the front (Fig. 1). This phenomenon occurs for a wide range of parameters and we describe a method that predicts the width of the band making this a natural target for future experimental study.

The CGLE in one space dimension is given by

$$\partial_t A = A + (1+ib)\partial_x^2 A - (1+ic)|A|^2 A, \qquad (1)$$

where the complex field A is a function of space x and time t, and b and $c>0$ are real parameters. This equation has a family of propagating front solutions connecting the unstable state $A=0$ to a plane wave. The latter is a fundamental class of solutions of the CGLE with the general form $A=\sqrt{1-Q^2}e^{iQx-i\omega t}$, where $\omega=(b+c)Q^2-c$ and $-1<Q<1$. Straightforward substitution reveals a one-parameter family of plane waves for all values of b and c. The wave number $Q(v)$ selected behind a propagating front is uniquely determined by the speed of the front v (which is $\geq 2\sqrt{1+b^2}$ [4]) via $v=(b-c)Q+(b+c)/Q$ [4,6]. Our specific focus is on the dynamics that results from the corresponding plane wave $A(v)$ being unstable. In such cases the plane-wave solution is either not observed or eventually undergoes a transition to more complex dynamics such as a pattern of localized defects or spatiotemporal chaos (Fig. 1).

In a previous study [7] we described and explained the phenomenon of fixed-width bands of plane waves in a system of reaction-diffusion equations of so-called "Lambda-Omega" type. These are simply CGLE (1) with the linear dispersion term $b=0$. Superficially, our results appeared to be qualitatively different from those of Nozaki and Bekki [6] and of subsequent authors (reviewed in [4]) for the full CGLE. These previous studies demonstrated the existence of a region of plane waves immediately behind the propagating front, whose width grows through time at a constant rate. However, when we performed longer term simulations of the full CGLE (1), we found this behavior to be a transient: the size of the region of plane-wave solutions eventually reaches a limit and remains at the limiting width for all subsequent times. Figure 1 illustrates three typical examples of the occurrence of plane-wave bands. In each case we apply a small initial perturbation localized near the left-hand boundary to the trivial state $A=0$. This induces a front to propagate across the domain. Behind the front there is a region of plane waves, whose width increases at early times, at a rate that can be calculated via the theory of linear spreading speeds [4,6]. However, in each case the long term behavior is a constant width plane-wave band.

In this paper we provide a detailed account of the occurrence and nature of the fixed-width band of plane waves in the CGLE. We first highlight some numerical errors in the study of Nozaki and Bekki [6] which led them to incorrect conclusions about the nature of the dynamics behind the

*http://research.microsoft.com/~mattsmi; matthew.smith@microsoft.com
†jas@ma.hw.ac.uk; http://www.ma.hw.ac.uk/~jas

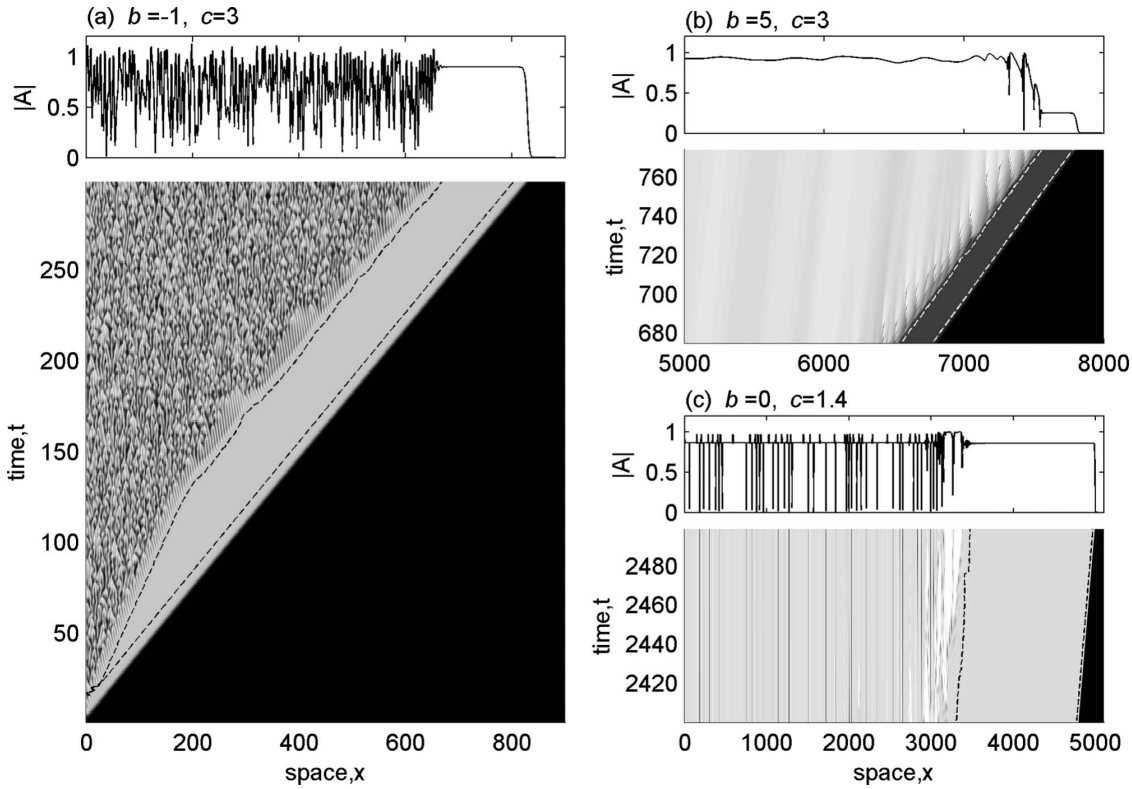

FIG. 1. Numerical simulations of pulled propagating fronts in CGLE (1) for different b and c values. The line plots show $|A|$ for the last time output of the surface plot below. The surface plots show the spatiotemporal dynamics of $|A|$ with darker shading indicating smaller $|A|$ and black corresponding to $|A|=0$. The dotted lines mark the beginning and end of the plane-wave band as detected using the method described in the main text. The figure shows that while different parameters can result in contrasting spatiotemporal dynamics behind the plane-wave band, the constant width of the band is a consistent phenomenon. Simulations are initialized with $|A|=0$ other than a small perturbation in $x<1$. The boundary conditions are $A_x=0$. Our numerical method is semi-implicit finite difference with grid spacing of 0.2 and a time step of 10^{-3}.

propagating front. Next we give a brief overview of the methods we used to predict the width of the plane-wave band. We then report our predictions for the parameter dependence of the width, which we confirm with simulations. Finally, we discuss likely physical systems that could be used to test our predictions.

II. CORRECTION TO THE STUDY OF NOZAKI AND BEKKI [6]

The first study that we are aware of on propagating fronts in the CGLE is that of Nozaki and Bekki [6]. These authors discuss fronts connecting the unstable background state to both stable and unstable plane waves. We began our own work by attempting to reproduce the numerical simulations in [6]. Despite [6] being very well cited, we found that the simulations contained previously unrecognized major qualitative errors due to problems with numerical truncation. This is most easily explained for Fig. 2 of [6], in which the authors show a propagating front, behind which there is a region of low amplitude plane waves, followed by plane waves of higher amplitude; both plane waves are stable. Moreover, the front shown in Fig. 2 of [6] undergoes a relatively abrupt change in speed part way through the simulation. The initial condition used in [6] is $\tilde{A}=\mathrm{sech}(0.05\tilde{x})$; here we use tildes to denote Nozaki and Bekki's variables, which differ from those in Eq. (1) via scalings. Our own simulations of this case show a uniformly propagating front followed by a single plane wave [Fig. 2(a)]. It seems that Nozaki and Bekki performed their computations in single precision. Thus, in reality they used initial conditions of the form $\tilde{A}=\mathrm{sech}(0.05\tilde{x})$ if $\mathrm{sech}(0.05\tilde{x})>10^{-5}$ and $\tilde{A}=0$ otherwise (the exact threshold would depend on details of their numerical implementation). In Fig. 2(b) we show the results of a simulation done at high precision but using this truncated initial condition, which reproduces Fig. 2 of Nozaki and Bekki. Figure 2(c) shows the results for $\tilde{A}(\tilde{x},0)=0$ apart from a perturbation localized to the left-hand boundary. In parts (a) and (c), a single stable wave train is selected behind the invasion front. However, the truncated initial conditions lead to a propagating front that is initially "pushed" before transitioning to a "pulled" front. These different propagating front speeds lead to two different plane-wave solutions being selected. The interface between these plane-wave bands gradually moves with the lower amplitude wave train replacing that of higher amplitude [19].

There is a similar problem in Fig. 3 of [6], which uses parameter values giving an unstable plane wave behind the front. In this case, the authors do not state their initial conditions explicitly, but the tacit implication is that again

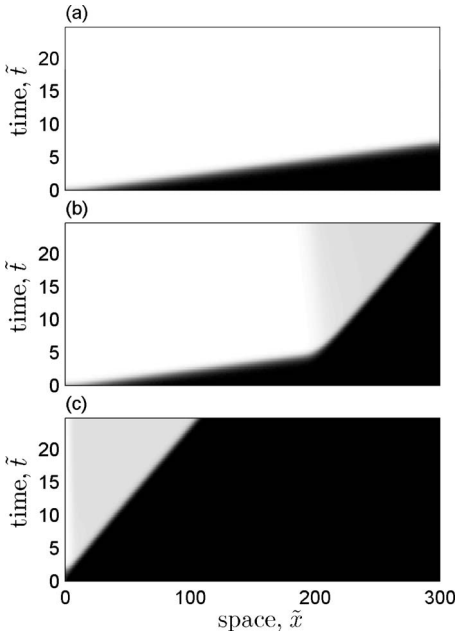

FIG. 2. Numerical solutions of the complex Ginzburg-Landau equation as formulated in Nozaki and Bekki [6] with parameters as in their Fig. 2. The equation is $\partial_{\tilde{t}}\tilde{A}=2\tilde{A}+(2.2+i)\partial_{\tilde{x}}^2\tilde{A}-(1+i)|\tilde{A}|^2\tilde{A}$, which can be converted to Eq. (1) by simple rescalings. Shading corresponds to the value of $|\tilde{A}|$, with darker shading indicating smaller $|\tilde{A}|$ and black corresponding to $|\tilde{A}|=0$. The initial conditions are as follows: (a) $\tilde{A}(\tilde{x},0)=\mathrm{sech}(0.05\tilde{x})$; (b) $\tilde{A}=\mathrm{sech}(0.05\tilde{x})$ if $\mathrm{sech}(0.05\tilde{x})>10^{-5}$ and $\tilde{A}=0$ otherwise; (c) $\tilde{A}(\tilde{x},0)=0$ except for a small perturbation near $\tilde{x}=0$. The boundary conditions are $\partial_{\tilde{x}}\tilde{A}=0$. Our numerical method is semi-implicit finite difference with grid spacing of 0.2 and a time step of 10^{-3}.

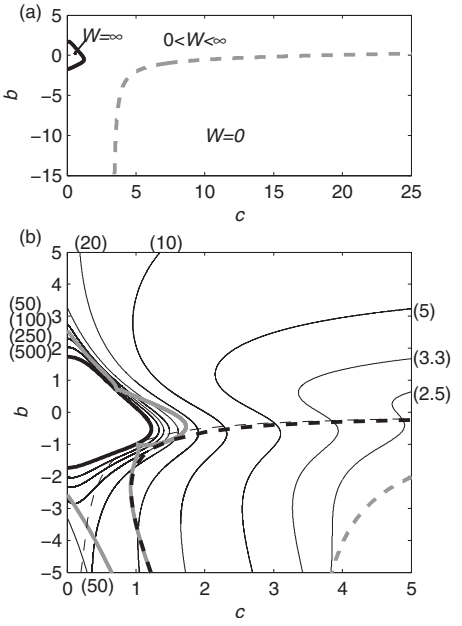

FIG. 3. (a) Wave train bands behind pulled propagating fronts in Eq. (1) are predicted to occur in (b,c) parameter space where $0<\mathcal{W}<\infty$. The gray broken line is the boundary at which the selected plane wave is absolutely unstable in the moving frame of reference with $V=v^*$. This line crosses the $b=0$ axis at $c=18.727\,51$. The thick solid line is the boundary at which the selected plane wave is stable. In (b) the thin black solid lines show contours for the bandwidth coefficient $\mathcal{W}$, with the coefficient values labeled at the edge of the plot, and we overlay the Benjamin-Feir-Newell curve (thin black broken line), the absolute instability curve (thick black broken line), and the absolute stability boundary (when $V=0$) for the plane wave selected by a pulled propagating front (thick gray line). There is a region of multiple $\mathcal{W}$ values in the bottom left of (b) located between the two $\mathcal{W}=50$ contours with $b<-2.5$.

$\tilde{A}(\tilde{x},0)=\mathrm{sech}(0.05\tilde{x})$. Again, we were able to reproduce their results by using the "truncated" version of this initial condition (we omit details for brevity). The rather complicated dynamics in Fig. 3(a) of Nozaki and Bekki is partly due to the truncated initial conditions generating different unstable plane waves in different parts of the domain. When Nozaki and Bekki were working, more than 25 years ago, computational precision was much more limited than today; nevertheless, care is still needed to avoid numerical artifacts when using initial conditions generating "pushed fronts." In Fig. 1 and throughout the remainder of this paper, we consider initial conditions that generate a "pulled front," which has asymptotic linear spreading speed $v^*=2\sqrt{1+b^2}$ [4]; we write $Q(v^*)=Q^*$ and $A(v^*)=A^*$ for brevity. However, we have also found the same phenomena in pushed fronts, for which the propagation speed is faster and the corresponding plane-wave solution is different.

Since Nozaki and Bekki's study there have been a number of real physical experiments that have reported the phenomenon of plane waves behind invasion fronts [4]. To our knowledge, however, none have studied the phenomenon in sufficient detail as to test our prediction that the growth of a plane-wave band is transient when the wave selected by the propagating front is unstable.

III. CALCULATING THE WIDTH OF THE PLANE-WAVE BAND

Our calculation of the width of the plane-wave band is based on methods we have used in previous studies of the dynamics behind propagating fronts in the case of $b=0$ [7,8]. We provide only a general overview here, concentrating on the elements that are different from our previous work, and refer the reader to our previous publications for detailed descriptions of the methodology.

The key issue underlying our calculation is the absolute stability of the plane wave A^* in a frame of reference moving with velocity V. If the plane wave is absolutely unstable in a frame with $V>v^*$, then perturbations to the plane wave can outrun the front and the plane wave will not be seen. Conversely, if the plane wave is stable then there will be an uninterrupted expanse of plane waves rather than a band. However, if the plane wave is convectively unstable in the frame of reference moving with the front speed v^* then all unstable modes will propagate away from the front as they grow leading to the band in which the plane waves are visible even though they are unstable. The left-hand edge of the band occurs when the perturbations present in the plane

wave immediately behind the front become sufficiently large that they dominate the plane wave itself, which we assume to occur when the perturbations become amplified by a scaling factor $\mathcal{F}$. For any given frame velocity V, the distance behind the front at which this amplification first occurs can easily be calculated: it depends on both the maximum growth rate of perturbations in that frame of reference and the speed $V-v^*$ at which the perturbation travels away from the front. The actual width of the plane-wave band is given by the V which minimizes this distance. In [7] we show that this is $V=V_{band}$, which solves

$$(v^* - V_{band})\mathrm{Im}[k_{max}(V_{band})] = \mathrm{Re}[\lambda_{max}(V_{band})], \qquad (2)$$

where λ_{max} is the growth rate of the most unstable linear mode and k_{max} is the corresponding spatial frequency. The bandwidth itself is $-\log(\mathcal{F})/\mathrm{Im}[k_{max}(V_{band})]$, so that all of the parameter dependence resides in $\mathcal{W}(b,c)=1/|\mathrm{Im}[k_{max}(V_{band})]|$, which we refer to as the "bandwidth coefficient." In general, there can be multiple solutions of Eq. (2) and it is then the smallest $\mathcal{W}$ that will determine the width of the plane-wave band.

There are three standard approaches to calculating absolute stability and, hence, λ_{max} and k_{max}: (i) numerical continuation of saddle points of $\lambda(k)-iVk$ in the complex k plane [9]; (ii) calculating the sign of the linear spreading speed [4]; (iii) calculating branch points in the absolute spectrum [10,11]. We adopt the last approach for which [11] gives a detailed methodological description. For a linear mode with temporal eigenvalue λ and spatial frequency k, the dispersion relation $\mathcal{D}(\lambda,k;V)=0$ is a quartic polynomial in k. We denote the four roots by $k_1,\ldots,k_4$ with $\mathrm{Im}\,k_1 \le \mathrm{Im}\,k_2 \le \mathrm{Im}\,k_3 \le \mathrm{Im}\,k_4$. "Branch points" are the (six) values of λ for which $k_i=k_{i+1}$ for some i and they are relevant to absolute stability if their index $i=2$, which corresponds to the "pinching condition" of [12]. Therefore, we solve Eq. (2) for V_{band} via numerical continuation of known solutions to

$$\mathcal{D}(\lambda,k;V) = \partial_k \mathcal{D}(\lambda,k;V) = 0 \qquad (3)$$

monitoring the indices of the repeated roots. Our numerical codes, which use the software packages MATLAB [13] and AUTO [14], are available from the first author on request. Note that our approach to calculating absolute stability concerns infinite domains, which is the relevant scenario for the plane-wave bandwidth. On bounded domains, plane-wave solutions of the CGLE can exhibit remnant instabilities in which perturbations grow while being repeatedly reflected from the boundaries [11,15], but such an instability is not relevant here.

We used MATLAB [13] to solve Eq. (3) for given values of b, c, and V giving six values of λ and their associated values of k. We used these values as starting points in numerical continuation of Eq. (3) in AUTO [14] for varying parameter values. We first performed continuations in V looking for values that satisfied Eq. (2). This then gave us V_{band} and, thus, λ_{max}, k_{max}, and $\mathcal{W}$ for given values of b and c. We next performed continuations in either b or c, while maintaining equality (2), to allow us to monitor the variation in $\mathcal{W}$ and to label combinations of b and c associated with specific values of $\mathcal{W}$. Finally, we used these labeled solutions as starting points for numerical continuations tracking contours of constant $\mathcal{W}$ in b-c parameter space.

We tested our predictions of $\mathcal{W}$ with numerical simulations of Eq. (1). We used a standard semi-implicit finite difference method to solve the equations (in MATLAB [13]). Numerical tests with this method showed that our simulations were accurate to about 0.1%. We used an automated method (implemented in MATLAB [13]) for detecting the width of the plane-wave band in simulations. We defined the observed bandwidth as the region immediately behind the invasion front at which $|\partial A/\partial x| < 1\times10^{-3}$. This condition gives a robust measure of bandwidth although the size of the threshold means that the resulting values are slightly smaller than (but directly correlated with) estimates suggested by visual inspection of space-time plots such as those shown in Fig. 1. We estimated the derivative numerically after applying a smoothing algorithm followed by a polynomial fit over a moving window of 9 grid points. By implementing this method we could then compare actual measures of bandwidth in numerical simulations with our predicted values of $\mathcal{W}$ from numerical continuation. We used standard linear regression to compare the predictions with the simulations. We allowed for nonzero intercepts in the regression lines because our method for measuring the width of the plane-wave band in simulations excludes some regions on either side.

Note that our defined threshold of $|\partial A/\partial x| < 1\times10^{-3}$ is larger than in our previous study of the $b=0$ case [7], where we used $|\partial A/\partial x| < 5\times10^{-7}$. We chose the new threshold because it resulted in a closer correspondence between the automated measurement and the size of the plane-wave band as visible by eye (as illustrated in Fig. 1). One consequence of the new threshold is that, as expected from our theory, it causes a change in the slope and intercept of the fitted linear relationship between observed bandwidth and $\mathcal{W}$; hence, these differ from those given in [7]. Repeating the analyses in [7] with the larger threshold results in estimates of the slope and intercept of the linear regression that are similar to those found here. This is consistent with our theory, which predicts that (for a given threshold) the observed bandwidth and $\mathcal{W}$ should be linearly related, with slope independent of the parameter values b and c.

IV. RESULTS

Our results indicate that a plane-wave band behind propagating fronts will occur for a wide range of parameter values in the CGLE [Fig. 3(a)]. As expected, one boundary to the parameter region in which a plane-wave band occurs is the contour at which the wave train band behind the propagating front becomes stable. Another boundary is the point at which the plane-wave band is absolutely unstable in all moving frame reference velocities, V. Along this curve, $V_{band}=v^*$ and $\mathcal{W}=0$.

Our analysis of $\mathcal{W}$ in (b,c) parameter space revealed the expected pattern of high bandwidth coefficients close to the plane-wave stability boundary with lower values further away [Fig. 3(b)]. It also revealed that the bandwidth varies nonmonotonically with parameters (see also Fig. 4). We also

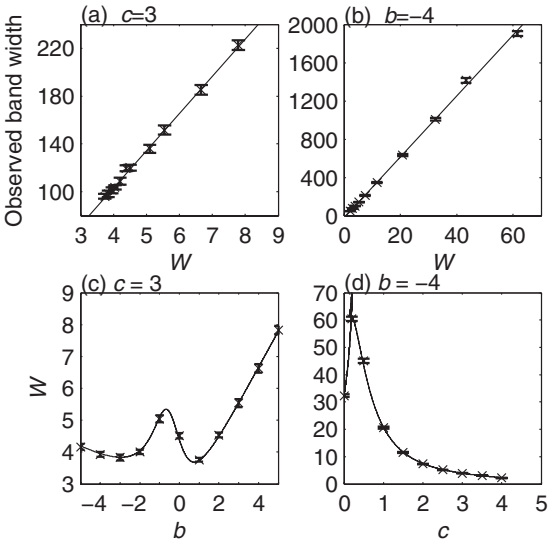

FIG. 4. Comparison of the bandwidth coefficient $\mathcal{W}$ with numerical simulations of Eq. (1). The initial and boundary conditions for the simulations are as in Fig. 1 except that the domain lengths and run times were set so that the region of plane-wave solutions behind the propagating front had reached its limiting width. The crosses and error bars show the mean and standard deviation of the observed plane-wave bandwidth for 100 solution times spaced one time unit apart. We also performed simulations with $(b,c)=(-4,4.5)$ and $(-4,5)$, which generated no plane-wave band, as predicted. (a) and (b) show the relationship between $\mathcal{W}$ and estimated plane-wave bandwidth from simulations. We superimpose the best-fit linear regression lines, which have slopes of 31.15 and 31.88, intercepts of −21.04 and −22.86, and correlation coefficients of 0.9921 and 0.9983, for (a) and (b), respectively. In (c) and (d) we have rescaled the measured plane-wave bandwidth using the linear regressions in (a) and (b). We chose equally spaced values of b or c for our simulations with the exception of one additional value at $c=0.2$ in (b) and (d), which we add to include a point close to the maximum in $\mathcal{W}$. A close-up of the region to the top left of (d) is given in Fig. 5(b). The lines in (c) and (d) are $\mathcal{W}$ values that were derived using the numerical continuation methods described in the main text. We measured the observed plane-wave bandwidth using the methods described in the main text.

plot in Fig. 3(b) the Benjamin-Feir-Newell curve (beyond which all plane-wave solutions are unstable), the absolute instability curve (beyond which all plane-wave solutions are absolutely unstable when $V=0$), and the absolute stability boundary for the plane wave selected by a pulled propagating front (when $V=0$). This highlights that these curves provide no real information about the bandwidth.

In Fig. 4 we compare the width of the plane-wave band observed in numerical simulations with $\mathcal{W}$ for two slices in the b-c parameter plane. The fit is extremely good. The figure also shows the nonmonotonic dependence of $\mathcal{W}$ on parameters.

We also discovered a region of multiple $\mathcal{W}$ values in the b-c parameter plane [Fig. 5(a)] which allowed us to test and confirm our prediction that it should be the smallest value of $\mathcal{W}$ [Fig. 5(b)] that determines the size of the plane-wave band. Although we did not find any other regions of multiple

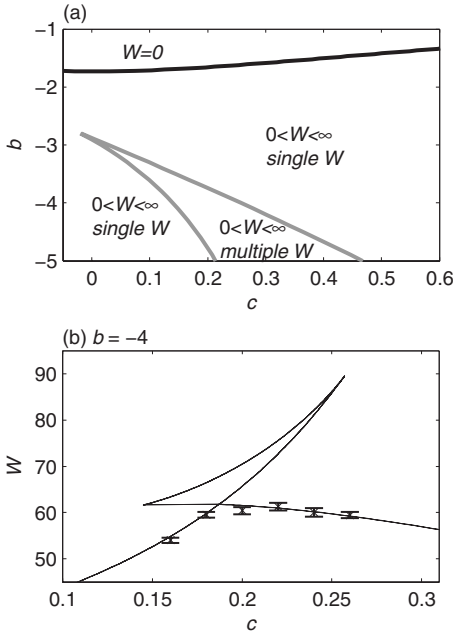

FIG. 5. (a) Wave train bands behind pulled propagating fronts in Eq. (1) are predicted to occur in (b,c) parameter space where $0<\mathcal{W}<\infty$. However, there are multiple $\mathcal{W}$ values in the region marked "multiple W." In such situations we predict that it is the smallest $\mathcal{W}$ value that determines the width of the plane-wave band. We include the contour at which $\mathcal{W}$ becomes zero to facilitate comparison with Fig. 3. (b) Numerical simulations confirm our prediction that, in the case of multiple $\mathcal{W}$ values, it is the smallest $\mathcal{W}$ value that determines the width of the plane-wave band. This is a close-up view of the region of multiple $\mathcal{W}$ values shown in Fig. 4(d) but with additional simulation results. See the legend of Fig. 4(d) for definitions. We used the same regression line as in Fig. 4(d) to rescale the measured bandwidth.

$\mathcal{W}$ values during our investigation, we do not know whether other such regions occur elsewhere in parameter space.

V. DISCUSSION

We have identified a phenomenon in the one-dimensional CGLE: fixed-width bands of plane waves behind propagating fronts. We have calculated the bandwidth as a function of parameters obtaining very good agreement with simulations. The constancy of the bandwidth over time and the ability to predict its value precisely make it a natural target for experiments. The widespread applicability of the CGLE means that there are a number of candidate systems that could be used. One such is convection in binary miscible fluids. At relatively high Rayleigh numbers, localized perturbations (in temperature) to the quiescent homogeneous conductive state can generate propagating fronts behind which are plane waves [16]. To our knowledge, only stable plane waves have been reported, but the relevant amplitude equation is the (cubic) CGLE [17] and, thus, our results suggest that plane-wave bands, followed by spatiotemporal chaos, would be found as control parameters are varied. Another possibility is the Taylor-Couette system with through flow [3] for which the (cubic) CGLE is again the relevant amplitude equation.

Localized perturbations can be generated by a sudden change in the inlet boundary location and lead to plane waves behind a propagating front. Previously, this has been used to locate the convective instability boundary, but its wider application would provide a natural test of our results. Potential nonphysical test systems include oscillatory chemical reactions [5] and oscillatory microbial interactions [18], both of which have been studied using the (cubic) CGLE. In all of these various cases, the relevant CGLE coefficients have already been derived, so that our results can be applied directly to predict the dependence of the width of the plane-wave band on the system parameters.

ACKNOWLEDGMENTS

We thank Jens Rademacher (CWI, Amsterdam) for many valuable discussions, Eric Hellmich, Robin Freeman, and Richard Mann (all Microsoft Research) for technical assistance, and Des Johnston (Heriot-Watt) for comments on the paper. J.A.S. was supported in part by the Leverhulme Trust.

[1] I. S. Aranson and L. Kramer, Rev. Mod. Phys. **74**, 99 (2002).
[2] A. C. Newell, in *Nonlinear Wave Motion*, edited by A. C. Newell (American Mathematical Society, Providence, RI, 1974); Y. Kuramoto, *Chemical Oscillations, Waves and Turbulence* (Springer-Verlag, Berlin, 1983).
[3] K. L. Babcock, G. Ahlers, and D. S. Cannell, Phys. Rev. Lett. **67**, 3388 (1991); A. Tsameret and V. Steinberg, Phys. Rev. E **49**, 4077 (1994).
[4] W. van Saarloos, Phys. Rep. **386**, 29 (2003).
[5] M. Cross and P. C. Hohenberg, Rev. Mod. Phys. **65**, 851 (1993); M. Ipsen, L. Kramer, and P. G. Sorensen, Phys. Rep. **337**, 193 (2000); A. S. Mikhailov and K. Showalter, *ibid.* **425**, 79 (2006).
[6] K. Nozaki and N. Bekki, Phys. Rev. Lett. **51**, 2171 (1983).
[7] J. A. Sherratt, M. J. Smith, and J. D. Rademacher, Proc. Natl. Acad. Sci. U.S.A. **106**, 10890 (2009).
[8] M. J. Smith, J. D. M. Rademacher, and J. A. Sherratt, SIAM J. Appl. Dyn. Syst. **8**, 1136 (2009).
[9] L. Brevdo, Z. Angew. Math. Mech. **75**, 423 (1995); L. Brevdo *et al.*, J. Fluid Mech. **396**, 37 (1999); S. A. Suslov, J. Comput. Phys. **212**, 188 (2006).
[10] B. Sandstede and A. Scheel, Physica D **145**, 233 (2000).
[11] J. D. M. Rademacher, B. Sandstede, and A. Scheel, Physica D **229**, 166 (2007).
[12] R. J. Briggs, *Electron-Stream Interaction with Plasmas* (MIT Press, Cambridge, USA, 1964); L. Brevdo, Geophys. Astrophys. Fluid Dyn. **40**, 1 (1988).
[13] The Mathworks, Version 7.6.0.324 (R2008a).
[14] E. J. Doedel, Congr. Numer. **30**, 265 (1981).
[15] D. Worledge, E. Knobloch, S. Tobias, and M. Proctor, Proc. R. Soc. London, Ser. A **453**, 119 (1997).
[16] P. Büchel and M. Lücke, Phys. Rev. E **63**, 016307 (2000).
[17] Ch. Jung, M. Lücke, and P. Büchel, Phys. Rev. E **54**, 1510 (1996).
[18] B. Kerr, M. A. Riley, M. W. Feldman, and B. J. M. Bohannan, Nature (London) **418**, 171 (2002); T. Reichenbach, M. Mobilia, and E. Frey, J. Theor. Biol. **254**, 368 (2008).
[19] R. Alvarez, M. van Hecke, and W. van Saarloos, Phys. Rev. E **56**, R1306 (1997); J. A. Sherratt, X. Lambin, and T. N. Sherratt, Am. Nat. **162**, 503 (2003); B. Sandstede and A. Scheel, SIAM J. Appl. Dyn. Syst. **3**, 1 (2004).